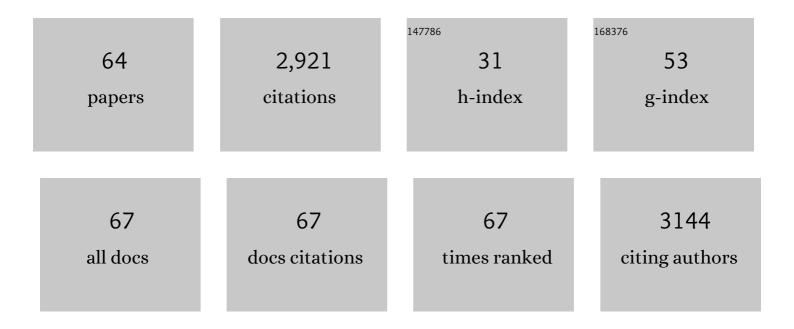
Yifang Ban

List of Publications by Year in descending order

Source: https://exaly.com/author-pdf/7836300/publications.pdf Version: 2024-02-01



VIEANC RAN

#	Article	IF	CITATIONS
1	Sentinel-1 and Sentinel-2 Data Fusion for Urban Change Detection Using a Dual Stream U-Net. IEEE Geoscience and Remote Sensing Letters, 2022, 19, 1-5.	3.1	26
2	Monitoring urbanization and environmental impact in Kigali, Rwanda using Sentinel-2 MSI data and ecosystem service bundles. International Journal of Applied Earth Observation and Geoinformation, 2022, 109, 102775.	1.9	7
3	Collaborative validation of GlobeLand30: Methodology and practices. Geo-Spatial Information Science, 2021, 24, 134-144.	5.3	31
4	Uni-Temporal Multispectral Imagery for Burned Area Mapping with Deep Learning. Remote Sensing, 2021, 13, 1509.	4.0	32
5	Learning U-Net without forgetting for near real-time wildfire monitoring by the fusion of SAR and optical time series. Remote Sensing of Environment, 2021, 261, 112467.	11.0	39
6	Dimensionality Reduction and Feature Selection for Object-Based Land Cover Classification based on Sentinel-1 and Sentinel-2 Time Series Using Google Earth Engine. Remote Sensing, 2020, 12, 76.	4.0	80
7	Continuous Monitoring of Urban Land Cover Change Trajectories with Landsat Time Series and LandTrendr-Google Earth Engine Cloud Computing. Remote Sensing, 2020, 12, 2883.	4.0	42
8	Near Real-Time Wildfire Progression Monitoring with Sentinel-1 SAR Time Series and Deep Learning. Scientific Reports, 2020, 10, 1322.	3.3	124
9	Dynamic Online 3D Visualization Framework for Real-Time Energy Simulation Based on 3D Tiles. ISPRS International Journal of Geo-Information, 2020, 9, 166.	2.9	18
10	Monitoring Urban Green Infrastructure Changes and Impact on Habitat Connectivity Using High-Resolution Satellite Data. Remote Sensing, 2020, 12, 3072.	4.0	22
11	Superpixel-Based Segmentation of Polarimetric SAR Images through Two-Stage Merging. Remote Sensing, 2019, 11, 402.	4.0	7
12	An implicit radar convolutional burn index for burnt area mapping with Sentinel-1 C-band SAR data. ISPRS Journal of Photogrammetry and Remote Sensing, 2019, 158, 50-62.	11.1	27
13	Monitoring of Urbanization and Analysis of Environmental Impact in Stockholm with Sentinel-2A and SPOT-5 Multispectral Data. Remote Sensing, 2019, 11, 2408.	4.0	19
14	Ship detection from PolSAR imagery using the ambiguity removal polarimetric notch filter. ISPRS Journal of Photogrammetry and Remote Sensing, 2019, 157, 41-58.	11.1	28
15	WorldView-2 Data for Hierarchical Object-Based Urban Land Cover Classification in Kigali: Integrating Rule-Based Approach with Urban Density and Greenness Indices. Remote Sensing, 2019, 11, 2128.	4.0	20
16	Urban land cover dynamics and their impact on ecosystem services in Kigali, Rwanda using multi-temporal Landsat data. Remote Sensing Applications: Society and Environment, 2019, 13, 234-246.	1.5	24
17	Unsupervised Difference Representation Learning for Detecting Multiple Types of Changes in Multitemporal Remote Sensing Images. IEEE Transactions on Geoscience and Remote Sensing, 2019, 57, 2277-2289.	6.3	36
18	Urban Land Cover and Ecosystem Service Changes based on Sentinel-2A MSI and Landsat TM Data. IEEE Journal of Selected Topics in Applied Earth Observations and Remote Sensing, 2018, 11, 485-497.	4.9	32

YIFANG BAN

#	Article	IF	CITATIONS
19	Adaptive Superpixel Generation for Polarimetric SAR Images With Local Iterative Clustering and SIRV Model. IEEE Transactions on Geoscience and Remote Sensing, 2017, 55, 3115-3131.	6.3	57
20	European Remote Sensing: progress, challenges, and opportunities. International Journal of Remote Sensing, 2017, 38, 1759-1764.	2.9	5
21	EO4Urban: Sentinel-1A SAR and Sentinel-2A MSI data for global urban services. , 2017, , .		14
22	Use of a geographic information system to identify differences in automated external defibrillator installation in urban areas with similar incidence of public out-of-hospital cardiac arrest: a retrospective registry-based study. BMJ Open, 2017, 7, e014801.	1.9	23
23	Superpixel Segmentation of Polarimetric SAR Images Based on Integrated Distance Measure and Entropy Rate Method. IEEE Journal of Selected Topics in Applied Earth Observations and Remote Sensing, 2017, 10, 4045-4058.	4.9	41
24	Sentinel-1A SAR and sentinel-2A MSI data fusion for urban ecosystem service mapping. Remote Sensing Applications: Society and Environment, 2017, 8, 41-53.	1.5	52
25	A novel approach for object-based change image generation using multitemporal high-resolution SAR images. International Journal of Remote Sensing, 2017, 38, 1765-1787.	2.9	22
26	Mapping and Monitoring Urban Ecosystem Services Using Multitemporal High-Resolution Satellite Data. IEEE Journal of Selected Topics in Applied Earth Observations and Remote Sensing, 2017, 10, 669-680.	4.9	30
27	Comparative Analysis on Topological Structures of Urban Street Networks. ISPRS International Journal of Geo-Information, 2017, 6, 295.	2.9	17
28	Route Choice of the Shortest Travel Time Based on Floating Car Data. Journal of Sensors, 2016, 2016, 1-11.	1.1	8
29	Multitemporal Remote Sensing: Current Status, Trends and Challenges. Remote Sensing and Digital Image Processing, 2016, , 1-18.	0.7	2
30	Change Detection Techniques: A Review. Remote Sensing and Digital Image Processing, 2016, , 19-43.	0.7	33
31	Fusion of Multitemporal Spaceborne SAR and Optical Data for Urban Mapping and Urbanization Monitoring. Remote Sensing and Digital Image Processing, 2016, , 107-123.	0.7	4
32	Unsupervised polarimetric SAR urban area classification based on model-based decomposition with cross scattering. ISPRS Journal of Photogrammetry and Remote Sensing, 2016, 116, 86-100.	11.1	59
33	Expanding the first link in the chain of survival – Experiences from dispatcher referral of callers to AED locations. Resuscitation, 2016, 107, 129-134.	3.0	31
34	Edge Detector for Polarimetric SAR Images Using SIRV Model and Gauss-Shaped Filter. IEEE Geoscience and Remote Sensing Letters, 2016, 13, 1661-1665.	3.1	22
35	The cross-scattering component of polarimetric SAR in urban areas and its application to model-based scattering decomposition. International Journal of Remote Sensing, 2016, 37, 3729-3752.	2.9	12
36	Model-Based Decomposition With Cross Scattering for Polarimetric SAR Urban Areas. IEEE Geoscience and Remote Sensing Letters, 2015, 12, 2496-2500.	3.1	57

YIFANG BAN

#	Article	IF	CITATIONS
37	Satellite monitoring of urbanization and environmental impacts—A comparison of Stockholm and Shanghai. International Journal of Applied Earth Observation and Geoinformation, 2015, 38, 138-149.	2.8	43
38	Spaceborne SAR data for global urban mapping at 30m resolution using a robust urban extractor. ISPRS Journal of Photogrammetry and Remote Sensing, 2015, 103, 28-37.	11.1	93
39	Real-time visualization of 3D city models at street-level based on visual saliency. Science China Earth Sciences, 2015, 58, 448-461.	5.2	8
40	Synergistic application of geometric and radiometric features of LiDAR data for urban land cover mapping. Optics Express, 2015, 23, 13761.	3.4	28
41	Predicting human mobility with activity changes. International Journal of Geographical Information Science, 2015, 29, 1569-1587.	4.8	34
42	Improving SAR-Based Urban Change Detection by Combining MAP-MRF Classifier and Nonlocal Means Similarity Weights. IEEE Journal of Selected Topics in Applied Earth Observations and Remote Sensing, 2014, 7, 4288-4300.	4.9	81
43	Exploring the relationship between street centrality and land use in Stockholm. International Journal of Geographical Information Science, 2014, 28, 1425-1438.	4.8	62
44	Urban growth and environmental impacts in Jing-Jin-Ji, the Yangtze, River Delta and the Pearl River Delta. International Journal of Applied Earth Observation and Geoinformation, 2014, 30, 42-55.	2.8	180
45	The evolving network structure of US airline system during 1990–2010. Physica A: Statistical Mechanics and Its Applications, 2014, 410, 302-312.	2.6	54
46	Multitemporal polarimetric RADARSAT-2 SAR data for urban land cover mapping through a dictionary-based and a rule-based model selection in a contextual SEM algorithm. Canadian Journal of Remote Sensing, 2013, 39, 138-151.	2.4	6
47	Generalization of 3D building texture using image compression and multiple representation data structure. ISPRS Journal of Photogrammetry and Remote Sensing, 2013, 79, 68-79.	11.1	11
48	Improving Urban Change Detection From Multitemporal SAR Images Using PCA-NLM. IEEE Transactions on Geoscience and Remote Sensing, 2013, 51, 2032-2041.	6.3	104
49	Multi-temporal RADARSAT-2 polarimetric SAR data for urban land-cover classification using an object-based support vector machine and a rule-based approach. International Journal of Remote Sensing, 2013, 34, 1-26.	2.9	113
50	Object-Based Fusion of Multitemporal Multiangle ENVISAT ASAR and HJ-1B Multispectral Data for Urban Land-Cover Mapping. IEEE Transactions on Geoscience and Remote Sensing, 2013, 51, 1998-2006.	6.3	61
51	Complex Network Topology of Transportation Systems. Transport Reviews, 2013, 33, 658-685.	8.8	151
52	Uncovering Spatio-Temporal Cluster Patterns Using Massive Floating Car Data. ISPRS International Journal of Geo-Information, 2013, 2, 371-384.	2.9	34
53	Range determination for generating point clouds from airborne small footprint LiDAR waveforms. Optics Express, 2012, 20, 25935.	3.4	22
54	Multitemporal RADARSAT-2 ultra-fine beam SAR data for urban land cover classification. Canadian Journal of Remote Sensing, 2012, 38, 1-11.	2.4	28

YIFANG BAN

#	Article	IF	CITATIONS
55	An empirical study on human mobility and its agent-based modeling. Journal of Statistical Mechanics: Theory and Experiment, 2012, 2012, P11024.	2.3	37
56	Nonlinear growth in weighted networks with neighborhood preferential attachment. Physica A: Statistical Mechanics and Its Applications, 2012, 391, 4790-4797.	2.6	10
57	Multitemporal Spaceborne SAR Data for Urban Change Detection in China. IEEE Journal of Selected Topics in Applied Earth Observations and Remote Sensing, 2012, 5, 1087-1094.	4.9	129
58	Satellite Monitoring of Urban Sprawl and Assessment of its Potential Environmental Impact in the Greater Toronto Area Between 1985 and 2005. Environmental Management, 2012, 50, 1068-1088.	2.7	28
59	Detection and typification of linear structures for dynamic visualization of 3D city models. Computers, Environment and Urban Systems, 2012, 36, 233-244.	7.1	24
60	A multiple representation data structure for dynamic visualisation of generalised 3D city models. ISPRS Journal of Photogrammetry and Remote Sensing, 2011, 66, 198-208.	11.1	48
61	Simulation and analysis of urban growth scenarios for the Greater Shanghai Area, China. Computers, Environment and Urban Systems, 2011, 35, 126-139.	7.1	109
62	Fusion of Quickbird MS and RADARSAT SAR data for urban land-cover mapping: object-based and knowledge-based approach. International Journal of Remote Sensing, 2010, 31, 1391-1410.	2.9	99
63	Synergy of multitemporal ERS-1 SAR and Landsat TM data for classification of agricultural crops. Canadian Journal of Remote Sensing, 2003, 29, 518-526.	2.4	77
64	Improving the Accuracy of Synthetic Aperture Radar Analysis for Agricultural Crop Classification. Canadian Journal of Remote Sensing, 1995, 21, 158-164.	2.4	12